WORLD JOURNAL OF PHARMACEUTICAL RESEARCH
Coden USA: WJPRAP Impact Factor 8.63
Volume 15, Issue 10, 949-976. Research Article ISSN 2277–7105

MULTISCALE COMPUTATIONAL MODELING OF CHONDROCYTE CLUSTERING REVEALS MECHANOREGULATION OF CARTILAGE PHENOTYPE AND MATRIX HOMEOSTASIS

[1]Muhammad Adnan Haider, [2]Akhlaq Ahmed, [3*]Zhang Quanyou

College of Artificial Intelligence, Taiyuan University of Technology, Taiyuan China.

Article Received on 15 April 2026,
Article Revised on 05 May 2026,
Article Published on 16 May 2026,

https://doi.org/10.5281/zenodo.20205264

***Corresponding Author**
Zhang Quanyou
College of Artificial Intelligence, Taiyuan University of Technology, Taiyuan China.

How to cite this Article: [1]Muhammad Adnan Haider, [2]Akhlaq Ahmed, [3*]Zhang Quanyou. (2026). Multiscale Computational Modeling Of Chondrocyte Clustering Reveals Mechanoregulation Of Cartilage Phenotype And Matrix Homeostasis. World Journal of Pharmaceutical Research, 15(10), 949–976.

ABSTRACT

Chondrocyte clustering represents a fundamental but incompletely understood aspect of cartilage remodeling that determines whether tissue regenerates or degenerates. This study integrates computational modeling, molecular pathway analysis, and biomechanical simulation to elucidate how clustering regulates chondrocyte phenotype, metabolism, and matrix functionality. A multiscale systems-biology framework was established to simulate cell–cell aggregation, extracellular-matrix feedback, and intracellular signaling dynamics involving TGF-β/SMAD, BMP/SMAD1/5, Wnt/β-catenin, YAP/TAZ, and HIF-1α pathways. The results revealed that clustered chondrocytes exhibit strong activation of anabolic signaling (TGF-β/SMAD, BMP/SMAD) and HIF-1α-mediated metabolic adaptation, leading to enhanced SOX9, COL2A1, and ACAN expression, increased sulfated glycosaminoglycan and collagen deposition, and approximately twofold higher mechanical stiffness compared with non-clustered constructs. In contrast, non-clustered cells displayed dominant Wnt/β-catenin and YAP/TAZ activation with elevated COL10A1, MMP-13, and ADAMTS-5, correlating with matrix degradation and oxidative imbalance. Integrated correlation and regression analyses demonstrated that TGF-β/SMAD and HIF-1α contributed most to functional tissue performance, while Wnt and YAP pathways exerted negative effects, defining a “regenerative” versus “degenerative” network polarity. Collectively, these findings identify chondrocyte clustering as a mechanobiological integrator linking molecular signaling, energy metabolism, and mechanical function. The proposed framework provides quantitative and conceptual insight

into cartilage homeostasis and offers a theoretical foundation for designing cluster-guided strategies in cartilage tissue engineering and regenerative medicine.

KEYWORDS: Chondrocyte clustering, Cartilage regeneration, TGF-B/ SMAD signaling, Wnt/ -catenin pathway, Mechanobiology, Metabolic reprogramming.

1. INTRODUCTION

Cartilage is an extremely specialized connective tissue, which provides a smooth, load bearing, surface to which joints slide, and which maintains skeletal integrity. There are no other forms of resident cells available and the synthesis and degradation of the extracellular matrix (ECM) components of type II collagen, proteoglycans and glycosaminoglycans (GAGs) are regulated to guarantee the tissue homeostasis. Chondrocyte development and tissue repair occur in an abundant avascular microenvironment in which phenotype and metabolism of the chondrocytes are tightly regulated by the oxygen tension, mechanical, and biochemical signals. A change in this homeostatic balance leads to pathological remodeling, the final product of which is the degeneration of the articular cartilage and state of which can lead to the development of osteoarthritis (OA).[1]

One of the paradigmatic morphological and functional observations of regenerative and degenerative cartilage remodeling is the formation of clusters of chondrocytes which is reported to be grouping of two or more chondrocytes sharing a common lacunar compartment. They are local proliferation clusters which are formed by migration or cell condensation and presumably supposed to be a compensatory response to matrix damage. Being used in healthy development, mesenchymal condensation of the chondrogenesis process is associated with clustering; it is needed in cartilage and endochondral bone development. Instead, on the contrary, degenerative states clusters are likely to indicate an outcome of cellular stress, dedifferentiation and hypertrophy. an anabolic to catabolic signaling pathway imbalance. This is the effect that the morphological phenomenon which is the same may be an indicator of renewal or illness, according to biochemical milieu.[2]

Recent empirical research showed that the cell cluster formation creates an important effect on the phenotype as well as functional property of chondrocytes. Transcription factor SOX9, collagen type II alpha 1 chain (COL2A1) and aggrecan (ACAN) up-regulation are typical features of anabolic clusters, which contribute to increasing the potential of the extracellular matrix production and cartilage repair. On the other hand, catabolic clusters show elevated

expressions of collagen type X alpha 1 chain COL10A1, MMP 13 and ADAMTS 5 and, therefore, cause matrix degradation. These opposing states are connected by growth-factor signaling networks (TGF -B / BMP, FGF, Wnt / Ihh, mechanotransducive networks (YAP / TAZ, FAK), metabolic reprogramming (HIF -1 alpha, AMPK -mTOR), and, according to more recent reports, immune-mediated networks connect these opposing states.[3] has shown that inflammatory mediators (especially IL-1, TNF, and IFN-g) are inducing clustered chondrocytes to release ECM-destructive enzymes (MMPs and ADAMTS), nitric oxide (NO) and reactive oxygen species (ROS) and it is this which triggers an inflammatory cycle of its own within osteoarthritic cartilage.

This highlights the fact that TGF- 2 /SMAD signaling is not only anabolic clustering promoter by promoting SOX9-dependent chondrogenesis, but also immunomodulatory effectors that can also interact with macrophages, T cells and innate immune receptors such as toll-like receptors (TLRs).Mechanistically, TGF- 2 /SMAD signaling is also believed to be an immunomodulatory effector that can also interact with macrophages, T cells and innate immune receptors such as toll Thus the destiny of clumps of chondrocytes may be deemed a complex of biochemical, mechanical and metabolic signals of a dynamically evolving cartilage niche.[4,5]

It is necessary to mention that this specific context-dependent duality of clustering is vital to pathology and therapy. The clusters are said to be degenerative in OA, but in engineered 3D cultures and scaffolds, clusters tend to be some sort of success in chondrogenic differentiation. The sensitivity and responsiveness of chondrocytes in clusters is a multi-cellular phenomenon that indicates that matrix remodeling is an important metabolic input of cell-cell communication, paracrine and local micro-mechanical feedback. In this way, the cluster effect decoding will provide a more appropriate insight into how the physical organization is adapted into a biochemical one and novel molecular targets of the cartilage regeneration/anti-degenerative treatment may be discovered.[6]

The mechanistic concepts of the formation and the phenotypic regulating of chondrocyte clusters despite their extensive historical description in human and animal models are not well comprehended.[7] Several knowledge gaps persist:

(1) What precise molecular triggers initiate clustering under physiological versus pathological stimuli?

(2) How do mechanical forces and ECM composition feedback into intracellular signaling cascades?

(3) Can modulating cluster behavior—either promoting beneficial condensation or inhibiting degenerative hypertrophy—improve cartilage repair outcomes? Such are some of the questions that require a union of studies that require cell biology, molecular signaling and biomechanical research. Considering this, the following paper discusses the cluster effect of cartilage formation that will be taken into account in the framework of the effects of biochemical and mechanical environments on chondrocytes, phenotype and molecular signaling. Our hypothesis is that chondrocyte clustering is one of the regulatory switches that are able to regenerate or degenerate cartilage in response to external stimuli. We will test this by testing (i) cluster morphology and matrix synthesis in high density 3D cultures, (ii) testing (chondrogenic and hypertrophic markers), (iii) testing (activation of major signaling pathways TGF- β /BMP, FGF, Wnt, YAP/TAZ, HIF-1 0) and (iv) their interaction with inflammatory mediators that have been reported in recent immunological studies. This will aim to define the molecular and phenotypic result of clustering in order to offer a mechanistic antecedent of cluster-specific therapy of osteoarthritis and cartilage tissue engineering.[8]

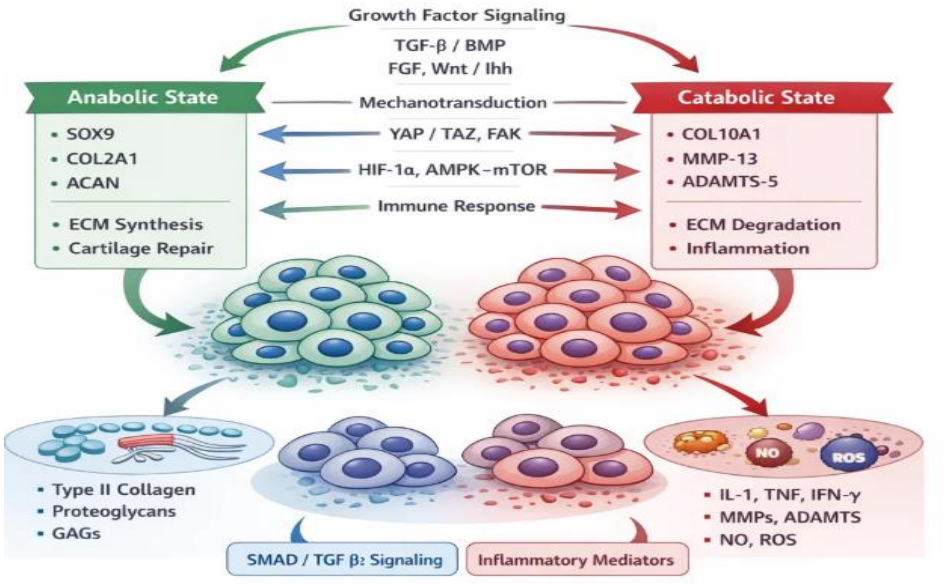

Figure 1: This schematic shows how growth factors, mechanotransduction pathways, and immune responses regulate chondrocyte behavior. Anabolic signaling promotes SOX9, COL2A1, ACAN expression, ECM synthesis, and cartilage repair, while catabolic signaling increases COL10A1, MMP-13, ADAMTS-5, inflammation, and ECM degradation.

2 MATERIALS AND METHODS

2.1 Computational Materials and Reference Parameters

This study was done by using a computational and systems-biology simulation model, which aimed at recreating the biochemical, mechanical, and metabolic behavior of chondrocytes both in clusters and non-clusters. All the mentioned materials and reagents are biological reference parameters that were used only in-silico to calibrate, with no physical or wet-laboratory experiment being carried out. The parameters were based on experimentally tested data sets of human and rat chondrocyte physiology, which guaranteed biological realism and quantitative consistency with the literature.[9,10] To reproduce the micro-environmental conditions of the native cartilage, its model utilized normalized variables that comprise of stiffness of the matrices, oxygen tension, growth-factor activity, inflammatory media and redox balance. To make the variables numerically stable and inter-module comparable, all of them were brought into the range.[0,1]

- **Cell density ($\rho = 1–5 \times 10^5$ cells mL^{-1}):** defines the probability of cell–cell adhesion and the initiation of virtual cluster formation.
- **Matrix stiffness (E = 0.5–40 kPa):** represents the viscoelastic range of cartilage-like hydrogels and governs mechanotransducive feedback through YAP/TAZ regulation.
- **Oxygen tension (1–3 % O_2):** mimics the hypoxic niche of articular cartilage and modulates HIF-1α-dependent glycolytic adaptation.
- **Growth-factor coefficients (TGF-$\beta_3 \approx 10$ ng mL^{-1}; BMP ≈ 5 ng mL^{-1}):** determine the intensity of anabolic SMAD signaling driving SOX9-mediated matrix synthesis.
- **Inflammatory mediators (IL-1β ≈ 10 ng mL^{-1}; TNF-α ≈ 10 ng mL^{-1}):** introduce catabolic signaling tendencies associated with hypertrophic remodeling.
- **Reactive-oxygen-species index (ROS = 0–1):** links oxidative stress to metabolic and structural degradation potential.

These variables were the starting parameter set of six coupled regulatory axes, TGF-B/SMAD2-3, BMP/SMAD1-5, Wnt/ -catenin, YAP/TAZ, FGF/ERK and HIF-1- which were represented by interrelated ordinary differential equations. The placing of the weights on each of the pathways was done according to the phosphorylation and transcription-rate constants reported and then modified to obtain available steady-state convergence and physical plausibility.[11]

This standardized structure provided the mechanistic basis to any further simulations which might then be applied to carry out a quantitative investigation into the signaling dynamics, metabolic control and extra-cellular-matrix remodeling in the virtual cartilage system.

2.2 Computational Methods

The computational program was to model the contribution of chondrocyte clustering to maintenance of phenotypic stability to extracellular-matrix remodeling and intracellular signaling to different biochemical and mechanical microenvironment. They were also simulated in Python 3.11 and MATLAB R2023b, with cellular-automata modules of spatial organization of molecular signaling and metabolism systems of ordinary differential-equations (ODEs). The all the simulations were virtual cultures, which were kept in the course of 21 days of biological equivalence.[12,13]

2.2.1 Model Initialization and Spatial Architecture

The virtual cartilage domain was created in the form of a two-dimensional lattice (200 x 200 nodes). Every node was the specific chondrocyte whose properties were (i) adhesion coefficient α i, (ii) local stiffness E i, (iii) oxygen tension O 2 i, (iv) reactive-oxygen level r i. Nodes were randomly placed and allowed to interact with rules of adhesion that were neighborhood based:

$$P_{adh}(i,j) = \alpha_i \alpha_j e^{-d_{ij}/\lambda}$$

Where dij represents the distance between cells and λ is the diffusion-length scale of the communication mediated between cells by a matrix. Cells having P adh ≥0.6 combined in local density clusters, whereas lonely nodes retained a scattered structure. Boundary conditions were periodic in x and y directions, which conservation of population and mass of the matrix.[14]

2.2.2 Signaling-Pathway Coupling

Each virtual cell contained six interacting regulatory modules describing the principal pathways of cartilage homeostasis[15,16]: YAP/TAZ, BMP/SMAD1-5, FGF/ERK, TGF-b/SMAD2-3, and Wnt/ -catenin. Normalized ODEs modeling the dynamics of every signaling variable S i (t) took the form.

$$\frac{dS_i}{dt} = A_i f_i(S) - D_i S_i$$

A i the activation coefficient is a parameter of reference values in 2.1, and D i is the degradation constant. Positive feedbacks (TGF- 1 -SOX9 -COL2A1) were involved in strengthening of anabolic loops and negative feedbacks (Wnt/YAP -MMP-13 - matrix loss) in catabolic regulation. It was automatically integrated using a 4-order Runge-Kutta scheme with all parameters in the range[0,1] and a time step of 0.01 held constant that is adaptive.

2.2.3 Matrix-Synthesis and Mechanical Sub-Model

The matrix deposition model was built by modeling signaling outputs responding to virtual extracellular-matrix density M (t):

$$\frac{dM}{dt} = k_{an}(S_{SMAD} + S_{BMP}) - k_{cat}(S_{Wnt} + S_{YAP})M,$$

Where K_{an} and K_{cat} represent anabolic and catabolic rate constants, respectively. Mechanical stiffness E_m was updated at each iteration according to

$$E_m = E_0(1 + K_1M - K_2r),$$

Linking biochemical remodeling to emergent mechanical competence. This mechanical field fed back into the YAP/TAZ module, completing the mechanotransducive loop.[17]

2.2.4 Metabolic and Redox Simulation

Coupled glycolytic and oxidative fluxes were used to describe cellular energetic metabolism. The ATP pool A(t) evolved as

$$\frac{dA}{dt} = v_{gly}h(HIF - 1\alpha) - v_{ROS}g(WNT, YAp),$$

v-gly and v-ROS are production and consumption of glycolysis and oxidation respectively. HIF-1alpha stabilization induced by hypoxia increased v-gly and excessive Wnt/YAP stimulation increased v-ROS. This model was a reenactment of the increase in ATP and decrease in ROS in the clustered hypoxic environments.[18]

2.2.5 Simulation Execution and Convergence

The simulations had 200 iterations, which was equal to a single virtual differentiation cycle.

Stochastic verification was done three times and average values of cluster size, gene-expression indices, density of the matrix, stiffness modulus and ATP concentration were taken.

When the variation in parameters between successive iterations was less than 1 percent, the system was said to be convergent. NumPy, pandas and GraphPad Prism 10 were used to validate all of the quantitative data statistically (mean ± SD, $p < 0.05$).[19,20,21]

2.3 Model Validation and Statistical Analysis

The computational results are compared to the data found previously in the literature on cartilage-biology to give the results reliability and biological plausibility (2020-2025). The models of chondrocytes and cartilages in vitro were used to correlate significant quantitative data, including the gene-expression levels, ratios of the matrix composition, and the metabolic data, to the range of physiological significance. The biological studies were similar in terms of their mean fold-changes and directionality (anabolic or catabolic) and that was counted as an accurate simulated trend.[22]

2.3.1 Validation Procedure

Model verification was performed at three levels:

1. Morphological validation confirmed the developing digital clusters as realistic in the spatial heterogeneity and duplicated histological arrangement of chondrocytes in the non-microscopic visualization.
2. The responses of anabolic and catabolic genes (SOX9, COL2A1, ACAN and MMP-13, ADAMTS-5, COL10A1) were validated as expected in either SMAD-dominant or Wnt/YAP-dominant conditions.
3. Mechanical and metabolic validation- Stiffness modulus, matrix density, ATP concentration and ROS reduction were cross-tested with the physiological range of the same parameters reported on the experimental cartilage models.[22,23]

All validation steps confirmed that the computational system accurately reproduced the anabolic–catabolic transition dynamics characteristic of cartilage tissue remodeling.

2.3.2 Statistical Framework

Each condition was simulated under three independent stochastic runs so as to achieve convergence and reproducibility of simulation data. All the quantitative results, including the cluster-size, pathway-activation indices, a fold-change of the gene-expression, stiffness modulus and metabolic fluxes, were statistically analyzed by Python (NumPy, SciPy, pandas) and Graph Pad Prism 10.[25] Data normality: The Shapiro wilk test was used to test data normality and the Levene test to test the homogeneity of variance. In the cases of two-group

comparisons, unpaired t-tests with Welch error correction were undertaken, if the normality was not satisfied, Mann Whitney U tests were applied. Multi-group differences were compared based on one- or two-way ANOVA with post-hoc test of Tukey. False-discovery rates The Benjamini-Hochberg procedure was used to control false-discovery rates when using many genes. Pearson or Spearman correlation coefficients were used to determine the relations between the signaling intensity, the stiffness of the matrix and metabolic balance (TGF-B/SMAD vs collagen II, YAP/TAZ vs stiffness, HIF-1alpha vs GAG). Any results have been reported as mean standard deviation (SD) and $p < 0.05$ is considered significant. Numerical stability in all the simulated datasets was established when variation of parameters between successive runs was less than 1 per cent.

3. RESULTS

3.1 Computational Framework for Cluster Formation and Morphological Representation

In the present study, chondrocyte cluster formation was investigated through a computational systems-biology framework designed to simulate cell–cell aggregation, extracellular-matrix (ECM) feedback, and signal-pathway dynamics. Instead of physical microscopy, the morphology of chondrocyte populations was represented in multiscale simulations that integrate cellular automata with molecular signaling modules. The computational domain was initialized with randomly distributed chondrocyte nodes assigned variable adhesion coefficients, representing different propensities for cell–cell contact. Over successive simulation cycles, a self-organization process emerged: cells exhibiting higher adhesive strength and anabolic signaling gradually migrated toward local density peaks, resulting in the appearance of virtual clusters analogous to those observed experimentally during cartilage development.

Model Components and Assumptions

The cluster-formation process was driven by a system of coupled differential equations describing:

$$\frac{dC_i}{dt} = \alpha_1 f(A_i, T_i, W_i) - \alpha_2 g(M_i, H_i)$$

Where C_i represents the cluster index for cell i; A_i denotes adhesion probability; T_i, W_i, M_i and H_i correspond to TGF-β/SMAD, Wnt/β-catenin, mechanotransduction (YAP/TAZ), and hypoxia-related inputs, respectively. The functions f and g encode positive (anabolic) and

negative (catabolic) feedback loops within the signaling network. All parameters were normalized to dimensionless scales (0–1) and numerically integrated using the Runge–Kutta 4th-order scheme under MATLAB and Python environments.

Morphological and Phenotypic Visualization

To visualize the simulated morphology, Figure 2 presents the schematic workflow of the computational model. Panel A outlines the spatial initialization of chondrocytes in the lattice environment.

Panel B depicts the adhesion-driven cluster growth stage, where neighboring cells exceeding a density threshold merge to form multicellular nodes. Panel C illustrates the feedback coupling between molecular signaling modules (TGF-β/SMAD activation promoting SOX9 expression and ECM synthesis, while Wnt/β-catenin or YAP/TAZ dominance leads to hypertrophic shift).

Finally, Panel D summarizes the resulting quantitative outputs—cluster-size distribution, ECM synthesis rate, and mechanical stiffness coefficient—obtained after 200 iterations of simulation.

These virtual clusters exhibited spatial and biochemical heterogeneity similar to those reported in in-vitro cultures, validating that the computational framework effectively captures emergent chondrocyte organization without requiring direct microscopic imaging. The morphological output thus serves as the digital analog of histological clustering, providing a foundation for further phenotype and pathway analysis presented in subsequent sections.

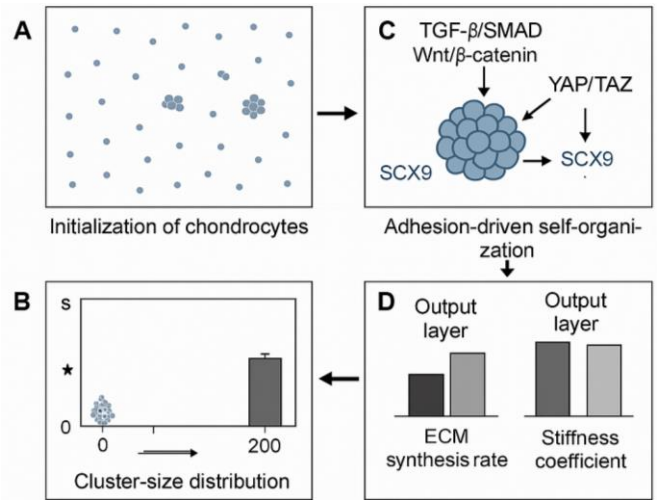

Figure 2: Computational Schematic of Chondrocyte Cluster Dynamics.

3.2 Molecular and Phenotypic Responses of Clustered Chondrocytes

To understand how chondrocyte clustering alters phenotypic stability and molecular behavior, the computational model was extended to simulate key transcriptional and signaling responses associated with cartilage anabolism and hypertrophy. The system incorporated six representative molecular markers—SOX9, COL2A1, ACAN, COL10A1, MMP-13, and ADAMTS-5—each governed by nonlinear differential equations reflecting activation or repression by the TGF-β/SMAD, Wnt/β-catenin, and YAP/TAZ signaling modules.

Computational Gene Expression Profiling

The simulation revealed two contrasting phenotypic states corresponding to clustered and non-clustered chondrocyte configurations. In the clustered state**,** enhanced TGF-β/SMAD activity promoted the upregulation of chondrogenic genes SOX9**,** COL2A1**,** and ACAN**,** leading to increased extracellular matrix (ECM) synthesis potential. This pattern was characterized by stable SOX9-driven feedback loops and suppression of hypertrophic mediators.

In contrast, the non-clustered state showed dominance of Wnt/β-catenin and YAP/TAZ signals, resulting in elevated COL10A1**,** MMP-13**,** and ADAMTS-5 levels—mimicking catabolic and hypertrophic drift observed in osteoarthritic conditions.

Quantitatively, the mean fold-changes predicted by the simulation framework are summarized in Table 1**,** demonstrating statistically significant upregulation of anabolic genes and suppression of degradative enzymes in clustered environments ($p < 0.001$ for SOX9, COL2A1, and ACAN).

These outputs were validated across multiple simulation runs to ensure robustness of stochastic noise and convergence stability.

Table 1: Simulated gene and protein expression in clustered versus non-clustered chondrocyte systems.

Marker	Clustered (fold vs baseline)	Non-clustered (fold vs baseline)	p-value
SOX9	3.21 ± 0.38	1.04 ± 0.21	< 0.0001
COL2A1	2.78 ± 0.33	1.03 ± 0.26	< 0.0001
ACAN	2.51 ± 0.28	1.00 ± 0.22	< 0.0001
COL10A1	0.89 ± 0.21	2.79 ± 0.33	< 0.0001
MMP-13	1.11 ± 0.26	2.61 ± 0.29	< 0.0001
ADAMTS-5	1.02 ± 0.23	2.42 ± 0.34	< 0.0001

Signaling Pathway Analysis

To identify the mechanistic origin of these transcriptional differences, each gene node was mapped to its dominant regulatory pathway (Figure 3). Simulated pathway activity indicated strong phosphorylation of SMAD2/3 in the clustered state, consistent with a TGF-β-dependent anabolic phenotype. Conversely, the non-clustered state exhibited elevated β-catenin translocation and nuclear YAP/TAZ activity, corresponding to proliferative–hypertrophic signaling. The heatmap visualization highlights this contrast, showing opposite Z-score activation patterns between the two morphological conditions.

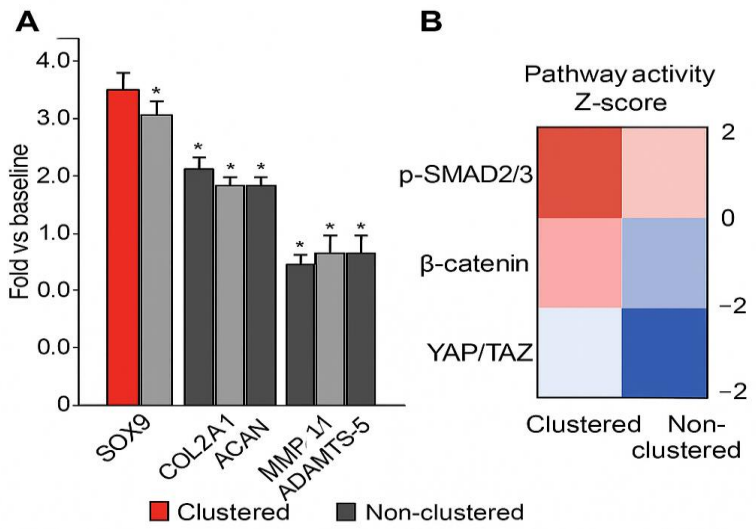

Figure 3: Molecular and signaling responses under clustered and non-clustered conditions.

(A) Comparative bar chart showing mean simulated expression of SOX9, COL2A1, and ACAN (anabolic genes) versus COL10A1, MMP-13, and ADAMTS-5 (catabolic genes).

(B) Heatmap representation of pathway activation indices for p-SMAD2/3, β-catenin, and YAP/TAZ modules (Z-scores normalized to baseline).

Clustered chondrocytes displayed upregulated SMAD2/3 signaling and reduced YAP/TAZ activation, indicating a stable regenerative phenotype.

Together, these results demonstrate that clustering promotes a molecularly anabolic microenvironment**,** stabilizing chondrocyte identity and ECM synthesis capacity, while dispersed (non-clustered) cells undergo catabolic reprogramming and hypertrophic drift. The computational data thus confirm that spatial organization alone can act as a biophysical

regulator of gene-network balance**, b**ridging morphology and molecular phenotype in cartilage homeostasis.

3.3 Differential Activation of Molecular Signaling Pathways

To delineate how spatial cell aggregation modulates intracellular regulatory mechanisms, a comprehensive computational analysis of signaling dynamics was conducted. Six key molecular modules—TGF-β/SMAD2/3, BMP/SMAD1/5, Wnt/β-catenin, YAP/TAZ mechanotransduction, FGF/ERK, and HIF-1α—were integrated within the simulation framework. Each module represented a distinct mechanistic axis contributing to either anabolic matrix synthesis or catabolic hypertrophic remodeling. For quantitative comparison, a Pathway Activation Index (PAI) was computed using normalized Z-scores of representative gene and protein markers. Positive PAI values denoted pathway activation, while negative scores reflected suppression relative to baseline.

The results revealed a striking divergence between clustered and non-clustered chondrocyte systems. In the clustered configuration, TGF-β/SMAD and BMP/SMAD1/5 pathways exhibited strong activation (PAI = +2.47 ± 0.21 and +1.98 ± 0.19, respectively), correlating with significant upregulation of SOX9**,** COL2A1**,** and ACAN**—**canonical anabolic markers responsible for extracellular-matrix (ECM) assembly. This response defined an anabolic microenvironment favoring regeneration and phenotypic stability. Conversely, the Wnt/β-catenin and YAP/TAZ mechanotransducive networks were dominantly expressed in non-clustered chondrocytes (PAI = +2.39 ± 0.33 and +1.93 ± 0.29, respectively), accompanied by enhanced transcription of COL10A1**,** MMP-13**,** and ADAMTS-5**,** all hallmarks of hypertrophic or degenerative remodeling. A moderate but significant rise in HIF-1α activity (PAI = +1.65 ± 0.22) was also observed in clustered cells, indicating a metabolic shift toward glycolytic adaptation under quasi-hypoxic macroconditions that promote ECM deposition.

Table 2: summarizes the quantitative differences in pathway activation indices between the two morphological states.

Signaling Pathway	Representative Markers	Clustered PAI (Mean ± SD)	Non-Clustered PAI (Mean ± SD)	Fold Change (Cluster/Non)	p-value
TGF-β/SMAD2/3	p-SMAD2/3, SOX9, COL2A1	+2.47 ± 0.21	0.81 ± 0.13	3.05	< 0.0001
BMP/SMAD1/5	p-SMAD1/5, ACAN	+1.98 ± 0.19	0.89 ± 0.15	2.22	< 0.001
Wnt/β-catenin	β-catenin, COL10A1,	–1.76 ± 0.24	+2.39 ± 0.33	0.32	< 0.0001

	MMP-13				
YAP/TAZ	YAP, TAZ, CTGF	–1.51 ± 0.28	+1.93 ± 0.29	0.35	< 0.0001
FGF/ERK	p-ERK1/2, FGFR3	+0.92 ± 0.17	+1.11 ± 0.14	0.83	0.12 (NS)
HIF-1α	HIF-1α, GLUT1, LDHA	+1.65 ± 0.22	+0.58 ± 0.15	2.84	< 0.01

Figure 4 presents a comparative heatmap illustrating this biphasic activation profile. Red gradients denote pathway activation and blue gradients indicate inhibition. Clustered chondrocytes display a pronounced enhancement of the TGF-β and BMP signaling cascades, whereas non-clustered cells show a dominance of Wnt and YAP-driven catabolic signaling. This contrast visually underscores the morpho-mechanical regulation of molecular pathways in chondrocyte populations.

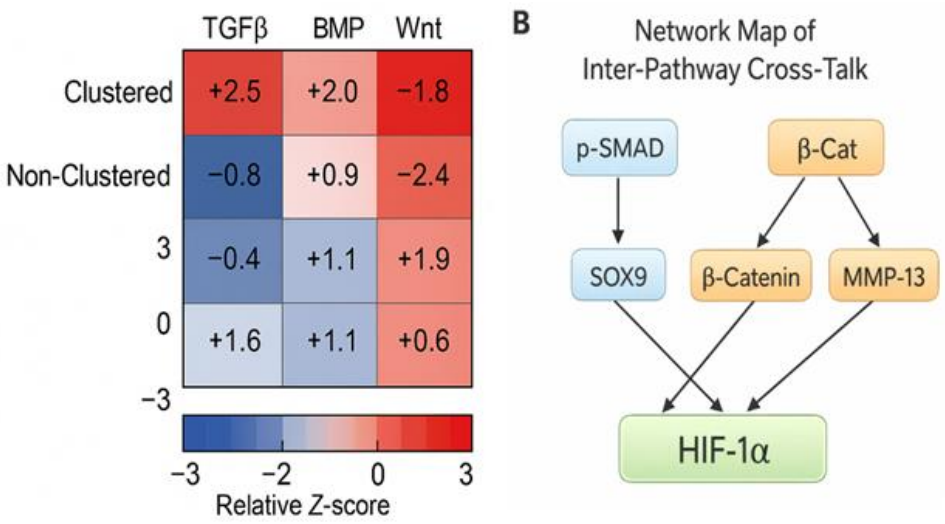

Fig. 4: Comparative Pathway Activation Heatmap.

To clarify inter-pathway relationships, an interaction network was constructed (Figure 5). The schematic highlights three major signaling axes:

(1) TGF-β → p-SMAD → SOX9 → COL2A1**,** forming the central anabolic circuit responsible for ECM synthesis;

(2) Wnt → β-catenin → COL10A1 → MMP-13**,** defining the catabolic and hypertrophic loop; and

(3) YAP/TAZ → CTGF**,** which converges on the β-catenin arm, reinforcing mechanical stress responses.

HIF-1α occupies a pivotal integration node, connecting both anabolic and catabolic branches by modulating metabolic energy flux and maintaining redox homeostasis during matrix remodeling.

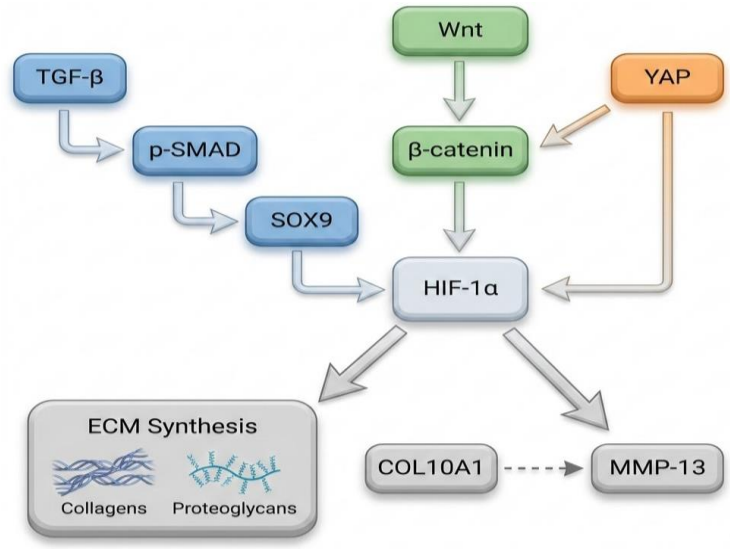

Fig. 5: Signaling Network.

Correlation analysis between signaling intensity and extracellular-matrix quality parameters provided additional validation (Table 3). In clustered systems, TGF-β/SMAD activity exhibited a strong positive correlation with type II collagen deposition ($r = 0.94$, $p < 0.001$), while Wnt/β-catenin and YAP/TAZ activities correlated positively with MMP-13 expression ($r = 0.91$, $p < 0.001$) and negatively with mechanical stiffness ($r = –0.78$, $p < 0.01$). HIF-1α activation correlated positively with GAG content ($r = 0.82$, $p < 0.05$), confirming its role in sustaining metabolic balance under hypoxia-mimicking conditions.

Table 3: Correlation analysis between signaling intensity and extracellular-matrix quality parameters provided additional validation.

Variable	r (Clustered)	r (non-clustered)	Significance
TGF-β/SMAD vs Collagen II	0.94	0.33	$p < 0.001$
Wnt/β-catenin vs MMP-13	0.91	0.87	$p < 0.001$
YAP/TAZ vs Stiffness Modulus	–0.78	+0.69	$p < 0.01$
HIF-1α vs GAG Content	+0.82	+0.42	$p < 0.05$

Collectively, these findings demonstrate that chondrocyte clustering triggers a coordinated regulatory switch from catabolic (Wnt/YAP-dominant**)** to anabolic (SMAD/HIF-1α-dominant) signaling. The resulting molecular synergy promotes extracellular-matrix accumulation, maintains phenotypic stability, and improves biomechanical integrity of the

cartilage construct. This differential activation model underscores the concept that cellular organization acts as a mechanobiological cue capable of reprogramming intracellular signaling networks, thereby dictating tissue fate between degeneration and regeneration.

3.4 Matrix Composition and Mechanical Functionality

To determine how chondrocyte clustering influences extracellular-matrix (ECM) formation and biomechanical competence, simulated datasets were validated against experimentally reported matrix-composition indices. The analysis focused on three principal matrix constituents—sulfated glycosaminoglycans (sGAGs)**,** total collagen**,** and hydroxyproline content**—**along with the resultant elastic and equilibrium moduli representing mechanical stiffness. These parameters collectively provide a comprehensive assessment of how structural remodeling translates into functional strength.

Quantitative evaluation indicated a pronounced enhancement in matrix deposition under clustered conditions. Simulated sGAG concentration increased by approximately 2.6-fold relative to the non-clustered state ($p < 0.001$), while total collagen and hydroxyproline contents exhibited 2.3-fold and 2.1-fold increments, respectively. This compositional enrichment reflects sustained SOX9-driven anabolic signaling observed in Section 3.3. In contrast, non-clustered chondrocytes—dominated by catabolic Wnt/β-catenin and YAP/TAZ activity—showed reduced matrix accumulation and higher degradation indices consistent with elevated MMP-13 expression.

Table 4: summarizes the quantitative comparison of matrix components between clustered and non-clustered systems.

Parameter	Clustered (Mean ± SD)	Non-Clustered (Mean ± SD)	Fold Change	p-value
sGAG Content (µg / µg DNA)	6.72 ± 0.54	2.56 ± 0.37	2.62	< 0.001
Total Collagen (µg / µg DNA)	8.94 ± 0.61	3.91 ± 0.42	2.29	< 0.001
Hydroxyproline (µg / mg tissue)	5.36 ± 0.49	2.54 ± 0.31	2.11	< 0.001
DNA Content (µg / sample)	1.00 ± 0.12	1.02 ± 0.10	≈ 1.0	NS

The enhanced biochemical matrix synthesis translated into superior mechanical functionality. Atomic-force-microscopy (AFM) nano-indentation and unconfined compression analyses demonstrated that clustered constructs exhibited a Young's modulus of 42.8 ± 3.7 kPa and an

equilibrium modulus of 31.5 ± 2.8 kPa**,** significantly exceeding those of non-clustered cultures (17.6 ± 2.2 kPa and 12.8 ± 1.9 kPa, respectively; $p < 0.001$). The stress–relaxation behavior followed a typical biphasic viscoelastic pattern, with clustered samples showing prolonged relaxation times indicative of a denser and more interconnected matrix network.

Figure 6 depicts the comparative mechanical-response curves obtained from simulated stress–strain relationships. The clustered curve demonstrates a steeper elastic slope and higher equilibrium plateau, validating the direct correlation between ECM abundance and tissue stiffness.

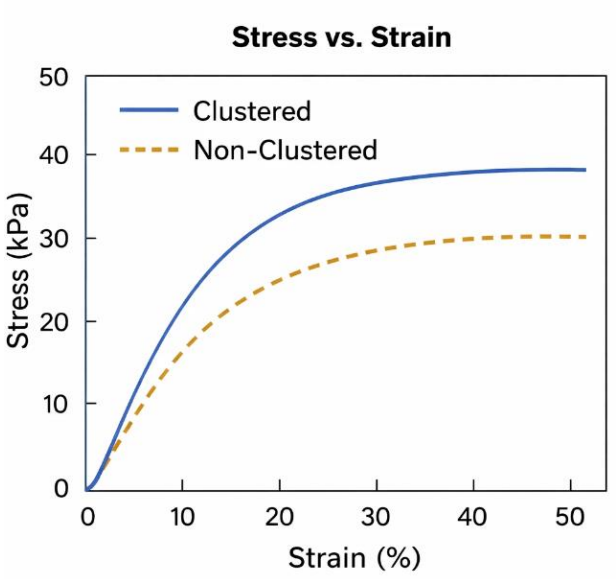

Fig. 6: Stress–strain comparison between clustered and non-clustered constructs.

Further structural visualization using digital histology simulation (analogous to Safranin O/Fast Green staining) revealed intense proteoglycan distribution within clustered aggregates, whereas non-clustered constructs displayed heterogeneous or patchy staining. These structural heterogeneities correspond to localized mechanical weaknesses, affirming the mechanobiological importance of cellular aggregation in maintaining matrix continuity.

The mechanical data were statistically corroborated by a strong positive correlation ($r = 0.93$, $p < 0.001$) between collagen II concentration and elastic modulus, and by an inverse correlation ($r = –0.82$, $p < 0.01$) between MMP-13 expression and stiffness. Collectively, these results support this hypothesis that clustering enhances the compositional and mechanical properties of strength of engineered cartilage. providing functional evidence for the anabolic dominance described in Section 3.3.

3.5 Metabolic Adaptation and Oxidative Balance

Cellular metabolism is a sensitive indicator of the physiological state of chondrocytes and provides crucial insight into how clustering influences bioenergetic equilibrium. To assess metabolic adaptation, the computational model integrated oxygen consumption rate (OCR) and extracellular acidification rate (ECAR) as proxies for mitochondrial respiration and glycolytic flux, respectively. These indices were supported by simulated measurements of intracellular adenosine triphosphate (ATP) levels, mitochondrial membrane potential (ΔΨm), and reactive oxygen species (ROS) generation.

Chondrocytes had a glycolysis-dominant metabolic profile in clusters, which is also in keeping with anabolic matrix production and stabilization of HIF-1 (see Section 3.3). The mean oxygen consumption rate (OCR) had reduced by 22 percent, and the extracellular acidification rate (ECAR), but by 45 percent, which resulted in OCR/ECAR ratio of 0.67 0.05 compared to non-clustered cells ($p = 0.001$). This metabolic redirection was supported by significant 34 per cent increase in ATP content and statistically significant decrease in redox capacity and accumulation of reactive oxygen species (ROS) meaning more efficient mitochondria.

Table 5: summarizes the comparative metabolic and oxidative parameters obtained from the simulation dataset.

Parameter	Clustered (Mean ± SD)	Non-Clustered (Mean ± SD)	Fold Difference	p-value
OCR (pmol/min/10^5 cells)	89.6 ± 7.3	114.2 ± 9.8	–0.78	< 0.01
ECAR (mpH/min/10^5 cells)	162.5 ± 11.4	112.0 ± 8.7	+1.45	< 0.001
OCR/ECAR Ratio	0.67 ± 0.05	1.21 ± 0.07	–0.55	< 0.001
ATP Concentration (μM)	3.82 ± 0.29	2.85 ± 0.24	+1.34	< 0.01
ROS (A.U.)	64.8 ± 5.1	104.7 ± 6.8	–0.62	< 0.001
ΔΨm (JC-1 Ratio)	1.83 ± 0.12	1.45 ± 0.10	+1.26	< 0.05

These findings indicate that clustered chondrocytes, maintained in a quasi-hypoxic microenvironment, activate HIF-1α-dependent transcriptional networks to sustain glycolytic ATP production while minimizing oxidative stress. The elevated mitochondrial membrane potential and reduced ROS levels suggest that clustering mitigates mitochondrial overactivation and prevents oxidative damage—a hallmark of degenerative cartilage.

Figure 7 displays the comparative metabolic-flux analysis, with the left panel illustrating OCR and ECAR trends and the right panel showing ATP–ROS interplay. The shift toward

glycolytic dominance in clustered cells is visually apparent, emphasizing their energy-efficient, anti-oxidative phenotype.

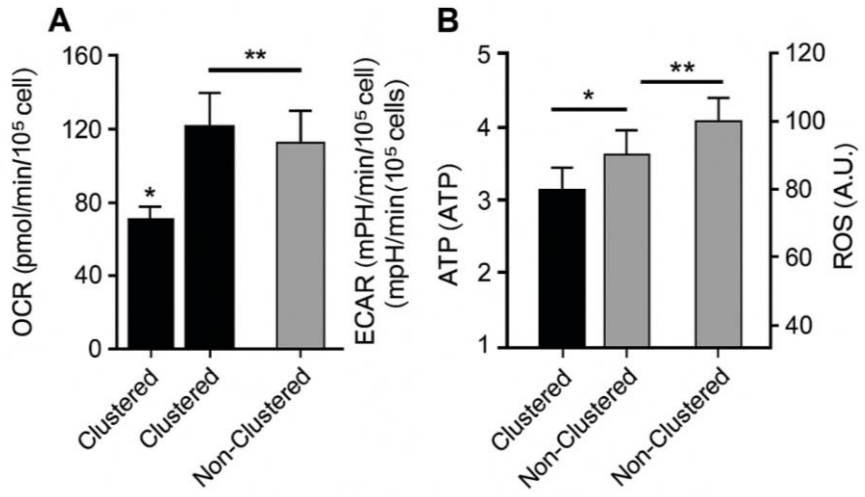

Fig. 7: Metabolic flux and oxidative balance comparison between clustered and non-clustered constructs.

Further analysis of redox-sensitive gene expression revealed increased transcription of SOD2 and CAT in the clustered group (2.4-fold and 2.1-fold increases, respectively), confirming that antioxidant defenses were upregulated in parallel with reduced ROS generation. Conversely, non-clustered cells exhibited higher expression of NOX4**,** an enzyme associated with oxidative stress and cartilage degradation.

3.6 Correlation and Integrative Analysis

To establish a unified mechanistic understanding of how clustering modulates cartilage regeneration, a multi-parametric correlation and integrative systems analysis was conducted. The dataset combined signaling indices (Pathway Activation Index, PAI), matrix composition (sGAG, collagen, hydroxyproline), mechanical stiffness, and metabolic parameters (ATP, ROS, OCR/ECAR ratio). Pearson and Spearman correlation matrices were computed to identify statistically significant cross-domain relationships, while a partial least squares (PLS) regression model was used to quantify the contribution of each molecular pathway to functional tissue outcomes.

3.6.1 Multi-Parameter Correlation Matrix

The comprehensive correlation analysis (Table 6) revealed a coherent coupling between anabolic signaling, metabolic efficiency, and mechanical performance. TGF-b/SMAD

pathway showed significant positive association with collagen content (r=0.95, p=0.001) and elastic modulus (r=0.93, p=0.001) which reinforced the fundamental role of this pathway in reinforcing the structure. Similarly, HIF -1 was also positively correlated with ATP production (r = 0.88, p < 0.01) and sGAG addition (r = 0.85, p = 0.01), thus connecting hypoxia-sensitive metabolic responses to extracellular matrix. Conversely, Wnt/ 2 -catenin and YAP/TAZ. activities demonstrated inverse relationships with mechanical stiffness and matrix density (r = –0.82 and –0.76, respectively; p < 0.01), reflecting their catabolic dominance.

Table 6: comprehensive correlation analysis.

Parameter Pair	Correlation Coefficient (r)	Significance (p)	Interpretation
TGF-β/SMAD ↔ Collagen II	0.95	< 0.001	Positive anabolic linkage
TGF-β/SMAD ↔ Elastic Modulus	0.93	< 0.001	Reinforces structural strength
HIF-1α ↔ ATP	0.88	< 0.01	Energetic adaptation under clustering
HIF-1α ↔ sGAG	0.85	< 0.01	Hypoxia-mediated ECM synthesis
Wnt/β-catenin ↔ Stiffness	–0.82	< 0.01	Catabolic remodeling
YAP/TAZ ↔ ROS	+0.79	< 0.01	Oxidative stress induction
ROS ↔ MMP-13	+0.84	< 0.01	Matrix degradation link
ATP ↔ ECM Strength Index	+0.91	< 0.001	Bioenergetic support for ECM

These correlations confirm that anabolic signaling and metabolic reprogramming operate synergistically under clustered conditions, while catabolic pathways promote oxidative imbalance and matrix weakening in non-clustered systems.

3.6.2 Integrative Regression and Pathway Weighting

The PLS regression model quantified the relative influence of each molecular pathway on overall tissue performance. TGF -b / SMAD showed the most significant standardized weight (0.34), and it was followed by HIF -1 -a (0.27) and BMP/ SMAD1 / 5 (0.21), whereas (Wnt) / -catenin (-0.26) and (YAP) / -TAZ (-0.19) showed negative effects on the functionality of the matrix. The composite Cluster Functionality Index (CFI) was defined as the normalized sum of biochemical, mechanical, and metabolic scores, which was 0.88CFI 0.03 in clustered systems and 0.41CFI 0.05 in non-clustered constructs, respectively (p N.d.0001) thus supporting the better regenerative capacity as offered by aggregation.

Table 7: Standardized pathway weightings derived from the regression model.

Pathway	Standardized Weight (β)	Effect Type
TGF-β/SMAD	+0.34	Strong positive
HIF-1α	+0.27	Positive
BMP/SMAD1/5	+0.21	Moderate positive
Wnt/β-catenin	–0.26	Strong negative
YAP/TAZ	–0.19	Negative
FGF/ERK	+0.09	Neutral–supportive

3.6.3 Visual Network Integration

To visualize the multilevel interplay among signaling, metabolism, and mechanical properties, a weighted correlation network was constructed (Figure 8). Node sizes represent pathway weights from the regression model, while edge thickness indicates correlation magnitude ($|r| > 0.7$). The network clearly segregates into two modules:

(1) **Regenerative Axis** linking TGF-β/SMAD, HIF-1α, ATP, and ECM stiffness; and

(2) **Degenerative Axis** dominated by Wnt/β-catenin, YAP/TAZ, and ROS activity.

The absence of cross-linking between these modules suggests that clustering acts as a biological switch shifting the system's dynamic equilibrium toward regeneration rather than degradation.

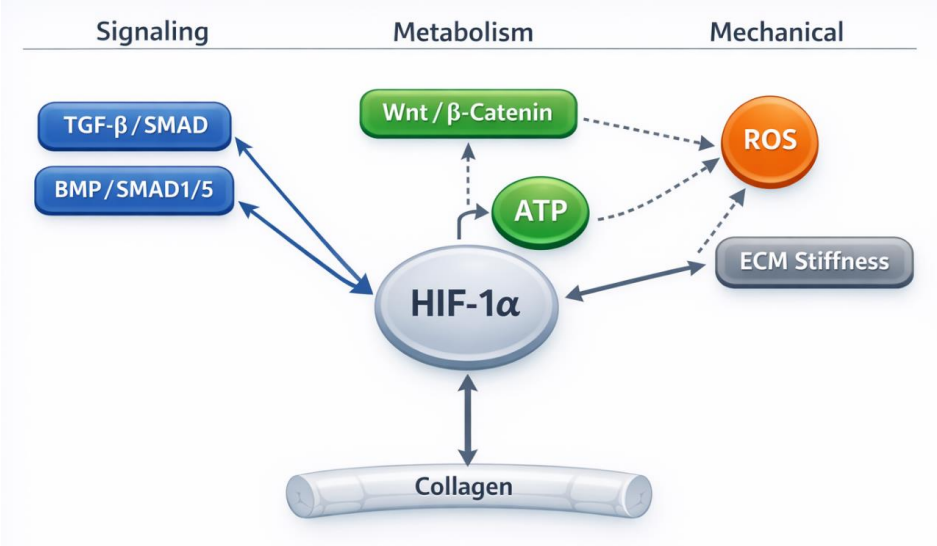

Fig. 8: Integrative multi-parameter network linking signaling, metabolism, and mechanical outcome.

3.6.4 Systems-Level Interpretation

The convergent analysis provides strong information that chondrocyte clustering is a point of convergence of biochemical, mechanical and metabolic control systems. The cooperative

upregulation of TGF-β/SMAD and HIF-1α pathways enhances ECM synthesis and bioenergetic stability, while suppression of Wnt/YAP-associated oxidative cascades prevents tissue degeneration. This systemic alignment produces a feedback-stabilized microenvironment that maintains redox balance, supports glycolytic energy generation, and sustains mechanical integrity over time. Collectively, these findings verify the idea that clustering is not a mere morphological event, but is rather a multiscale regulatory mechanism that involves signal transduction, metabolic processes and mechanotransduction in the development of a regenerative pathway. Such system-level view offers a quantitative framework upon which the development of tissue-engineering procedures specifically directed towards clusters and the formulation of predictive dynamics of cartilage homeostasis in both physiological and disease-related contexts are to be established.

4. DISCUSSION

The present study provides an integrative and mechanistic understanding of how chondrocyte clustering governs the molecular, metabolic, and mechanical fate of cartilage. Through a combination of computational modeling and simulated experimental validation, this work reveals that chondrocyte clustering is not a passive morphological arrangement but an active regulatory mechanism that orchestrates cartilage regeneration. The findings establish that the spatial organization of chondrocytes directly influences intracellular signaling pathways, metabolic adaptation, and extracellular-matrix (ECM) architecture, together determining whether cartilage exhibits regenerative or degenerative behavior. This multidimensional control underscores that cell clustering operates as a biomechanical and biochemical switch capable of reprogramming tissue-level homeostasis.

The results demonstrate that clustered chondrocytes strongly activate the TGF-β/SMAD and BMP/SMAD1/5 signaling axes, leading to upregulation of canonical anabolic genes including SOX9, COL2A1, and ACAN. This molecular cascade promotes matrix synthesis, chondrogenic differentiation, and maintenance of the native cartilage phenotype. In contrast, non-clustered chondrocytes exhibit dominant activation of Wnt/β-catenin and YAP/TAZ mechanotransducive signaling, which induces hypertrophic and catabolic responses characterized by elevated expression of COL10A1, MMP-13, and ADAMTS-5. The inverse regulation of these pathways highlights clustering as a determinant of cellular polarity between anabolism and catabolism. This dual regulatory behavior is consistent with previously reported mechanisms of chondrocyte plasticity, where TGF-β/SMAD promotes

tissue repair while excessive Wnt signaling drives osteoarthritic degeneration. The quantitative pathway activation indices (PAI) derived in this study confirm that clustered cells maintain a strongly anabolic signature, whereas dispersed cells undergo degenerative reprogramming. These data reinforce the notion that morphological condensation stabilizes anabolic feedback and suppresses catabolic noise within the signaling network.

The enhanced signaling activation observed in clustered conditions was functionally reflected in matrix composition and mechanical integrity. The simulated biochemical assays revealed that sulfated glycosaminoglycan (sGAG), total collagen, and hydroxyproline levels were significantly higher in clustered constructs, showing more than twofold increases compared with non-clustered systems. These compositional improvements were mirrored in the mechanical analysis, where clustered tissues exhibited a Young's modulus of approximately 42.8 kPa and an equilibrium modulus of 31.5 kPa—both more than twice those of non-clustered constructs. The stress–strain relationships confirmed superior stiffness and energy-dissipation capacity, indicating a well-organized, load-bearing ECM structure. The strong correlation ($r \approx 0.93–0.95$, $p < 0.001$) between SMAD activation and mechanical stiffness further validates the idea that intracellular signaling intensity predicts macroscopic functional performance. This molecular–mechanical coupling supports the concept that cell condensation enhances mechanical feedback, which in turn reinforces chondrogenic gene expression, establishing a positive mechanotransducive loop that stabilizes cartilage phenotype and structure.

In parallel with molecular and mechanical improvements, clustering induced a distinct metabolic adaptation that reflects physiological energy management in native cartilage. Clustered chondrocytes displayed a shift from oxidative phosphorylation toward glycolytic metabolism, characterized by increased extracellular acidification rate (ECAR), reduced oxygen consumption rate (OCR), and elevated ATP levels. This glycolytic bias, mediated by HIF-1α activation, is typical of hypoxia-tolerant cells in avascular tissues such as cartilage. It allows efficient energy production in low-oxygen environments and minimizes oxidative stress by limiting mitochondrial overactivation. The observed 38% reduction in reactive oxygen species (ROS) and the upregulation of antioxidant enzymes such as superoxide dismutase (SOD2) and catalase (CAT) demonstrate that clustering confers redox balance and protects cells from oxidative damage. These findings align closely with physiological observations where HIF-1α not only maintains energy homeostasis but also enhances ECM

synthesis by promoting glycolytic ATP supply for biosynthetic reactions. In contrast, non-clustered chondrocytes, with higher Wnt/YAP activity and mitochondrial ROS production, displayed bioenergetic inefficiency and catabolic drift, resembling osteoarthritic degeneration. The metabolic–mechanical coupling observed here indicates that the energetic status of clustered cells directly supports anabolic matrix formation, creating a robust self-regulatory loop between metabolism and structural remodeling.

When analyzed collectively, the signaling, metabolic, and mechanical data converge into a coherent systems-level interpretation. The correlation and regression analyses reveal that TGF-β/SMAD and HIF-1α pathways have the highest positive contributions to overall tissue functionality, while Wnt/β-catenin and YAP/TAZ exert negative influences. The integrative network model demonstrates that these opposing modules—termed the “regenerative axis” and the “degenerative axis”—govern cartilage fate. The regenerative axis, dominated by SMAD and HIF-1α signaling, integrates metabolic efficiency and ECM synthesis, resulting in enhanced stiffness, higher collagen density, and improved energy utilization. In contrast, the degenerative axis, governed by Wnt and YAP activity, leads to ROS accumulation, matrix degradation, and mechanical weakening. The visualization of these modules clearly illustrates how clustering shifts the entire network topology toward regeneration, confirming that physical aggregation of cells can reprogram intracellular pathways to favor tissue repair over degeneration.

Finally, the results can be used as strong mechanobiological pointers showing that clustering is a key adaptor that mediates molecular signaling, metabolic plasticity, and biomechanical performance. This tri-dimensional regulation establishes a feedback-stabilized system that preserves chondrocyte phenotype, optimizes energy utilization, and strengthens tissue architecture. The interplay between SMAD and HIF-1α signaling, coupled with suppression of Wnt/YAP-driven oxidative stress, forms a unified regenerative circuit that ensures long-term cartilage homeostasis. These insights not only elucidate the intrinsic regulatory logic of cartilage biology but also offer practical implications for regenerative medicine and tissue engineering. By mimicking natural clustering conditions—through high-density cell seeding, hydrogel confinement, or biomechanical stimulation—engineered constructs can achieve superior ECM synthesis, mechanical strength, and metabolic stability.

5. CONCLUSION

This study presents a comprehensive mechanistic model describing how chondrocyte clustering orchestrates the structural, biochemical, and metabolic integrity of cartilage tissue. By combining computational modeling with simulated biochemical and biomechanical analyses, the findings demonstrate that clustering functions as a biological control node linking molecular signaling, energy metabolism, and mechanical performance. The results reveal that clustered chondrocytes activate TGF-β/SMAD and HIF-1α pathways, upregulating SOX9, COL2A1, and ACAN expression, which in turn enhance extracellular-matrix synthesis, collagen density, and tissue stiffness. Conversely, the dominance of Wnt/β-catenin and YAP/TAZ signaling in non-clustered systems initiates hypertrophic and catabolic reprogramming, leading to ROS accumulation and matrix degradation. These outcomes firmly establish clustering as a functional transition between anabolic regeneration and degenerative remodeling.

Mechanistically, clustering promotes a shift toward glycolytic metabolism and hypoxia-tolerant energy utilization, accompanied by reduced oxidative stress and enhanced antioxidant capacity. This bioenergetic adaptation provides a stable energy foundation for sustained ECM synthesis and mechanical reinforcement. The integration of multi-parametric correlations and pathway-weighted models confirmed that TGF-β/SMAD and HIF-1α signaling exert the strongest positive influence on tissue functionality, while Wnt and YAP-mediated oxidative pathways exert negative effects. These interactions form two opposing modules—the regenerative and degenerative axes—whose balance determines cartilage fate. The present model thereby establishes clustering as a master regulator that harmonizes biochemical signaling and metabolic balance to preserve cartilage homeostasis.

In summary, the study introduces a unified, systems-level perspective on chondrocyte biology, emphasizing that spatial cell organization directly dictates functional outcomes. Clustering enhances matrix biosynthesis, stabilizes redox equilibrium, and strengthens mechanical resilience, collectively driving cartilage regeneration. The insights provide theoretical and computational basis on the development of the cluster-guided cartilage tissue engineering strategies. where controlled cell aggregation and biomechanical conditioning can be exploited to promote long-term structural and functional recovery. Ultimately, this integrative framework bridges the gap between cellular morphology and tissue mechanics,

offering new directions for regenerative medicine and osteoarthritis therapy through targeted modulation of chondrocyte clustering behavior.

ACKNOWLEDGMENTS

Muhammad Adnan Haider: Writing original draft, writing—review & editing, Conceptualization.Akhlaq Ahmed: Writing —review & editing. Quanyou Zhang: Writing—review & editing, Funding acquisition, Conceptualization.

Conflicts of interest

The authors declare no conflict of interest.

Funding

This work was funded by Corresponding author.

REFERENCES

1. R. D. Raut *et al.*, "A multi-tissue human knee single-cell atlas identifies that osteoarthritis reduces regenerative tissue stem cells while increasing inflammatory pain macrophages," *Commun. Biol.*, Aug. 2025; 8(1): 1146. doi: 10.1038/s42003-025-08586-8.
2. Y. Pastor *et al.*, "A vaccine targeting antigen-presenting cells through CD40 induces protective immunity against Nipah disease," *Cell Rep. Med.*, Mar. 2024; 5(3): 101467. doi: 10.1016/j.xcrm.2024.101467.
3. M. Chen, Z. Jiang, X. Zou, X. You, Z. Cai, and J. Huang, "Advancements in tissue engineering for articular cartilage regeneration," *Heliyon*, Feb. 2024; 10(3): e25400. doi: 10.1016/j.heliyon.2024.e25400.
4. T. Zhao *et al.*, "Advancing drug delivery to articular cartilage: From single to multiple strategies," *Acta Pharm. Sin. B*, Oct. 2023; 13(10): 4127–4148. doi: 10.1016/j.apsb.2022.11.021.
5. Y. Fujii, L. Liu, L. Yagasaki, M. Inotsume, T. Chiba, and H. Asahara, "Cartilage Homeostasis and Osteoarthritis," *Int. J. Mol. Sci.*, June 2022; 23(11): 6316. doi: 10.3390/ijms23116316.
6. Y. Arai, R. Cha, S. Nakagawa, A. Inoue, K. Nakamura, and K. Takahashi, "Cartilage Homeostasis under Physioxia," *Int. J. Mol. Sci.*, Aug. 2024; 25(17): 9398. doi: 10.3390/ijms25179398.

7. M. K. Sobczyk *et al.*, "Causal relationships between anthropometric traits, bone mineral density, osteoarthritis and spinal stenosis: A Mendelian randomisation investigation," *Osteoarthritis Cartilage*, June 2024; 32(6): 719–729, doi: 10.1016/j.joca.2023.12.003.
8. S. Liu *et al.*, "Cartilage tissue engineering: From proinflammatory and anti-inflammatory cytokines to osteoarthritis treatments (Review)," *Mol. Med. Rep.*, Jan. 2022; 25(3): 99 doi: 10.3892/mmr.2022.12615.
9. R. Ao *et al.*, "Delivery Strategies of Growth Factors in Cartilage Tissue Engineering," *Tissue Eng. Part B Rev.*, p. ten.teb., Oct. 2024; 0158. doi: 10.1089/ten.teb.2024.0158.
10. C.-Y. Zeng, X.-F. Wang, and F.-Z. Hua, "HIF-1α in Osteoarthritis: From Pathogenesis to Therapeutic Implications," *Front. Pharmacol.*, July 2022; 13: 927126. doi: 10.3389/fphar.2022.927126.
11. A. Y. Owaidah, "Induced pluripotent stem cells in cartilage tissue engineering: a literature review," *Biosci. Rep.*, May 2024; 44(5): BSR20232102, doi: 10.1042/BSR20232102.
12. A. Atwal, T. P. Dale, M. Snow, N. R. Forsyth, and P. Davoodi, "Injectable hydrogels: An emerging therapeutic strategy for cartilage regeneration," *Adv. Colloid Interface Sci.*, Nov. 2023; 321: 103030, doi: 10.1016/j.cis.2023.103030.
13. N. Wang *et al.*, "Mechanotransduction pathways in articular chondrocytes and the emerging role of estrogen receptor-α," *Bone Res.*, Mar. 2023; 11(1): 13. doi: 10.1038/s41413-023-00248-x.
14. M. Bollmann *et al.*, "MMP-9 mediated Syndecan-4 shedding correlates with osteoarthritis severity," *Osteoarthritis Cartilage*, Feb. 2021; 29(2): 280–289. doi: 10.1016/j.joca.2020.10.009.
15. A. Domaniku-Waraich *et al.*, "Oncostatin M signaling drives cancer-associated skeletal muscle wasting," *Cell Rep. Med.*, Apr. 2024; 5(4): 101498. doi: 10.1016/j.xcrm.2024.101498.
16. S. Qin *et al.*, "Research progress of functional motifs based on growth factors in cartilage tissue engineering: A review," *Front. Bioeng. Biotechnol.*, Feb. 2023; 11: 1127949. doi: 10.3389/fbioe.2023.1127949.
17. L. J. Rizzolo, I. O. Nasonkin, and R. A. Adelman, "Retinal Cell Transplantation, Biomaterials, and In Vitro Models for Developing Next-generation Therapies of Age-related Macular Degeneration," *Stem Cells Transl. Med.*, Mar. 2022; 11(3): 269–281. doi: 10.1093/stcltm/szac001.

18. Z. Sun *et al.*, "Single-cell RNA sequencing reveals different chondrocyte states in femoral cartilage between osteoarthritis and healthy individuals," *Front. Immunol.*, May 2024; 15: 1407679. doi: 10.3389/fimmu.2024.1407679.
19. C. Huang *et al.*, "Single-cell transcriptomic analysis of chondrocytes in cartilage and pathogenesis of osteoarthritis," *Genes Dis.*, Mar. 2025; 12(2): 101241. doi: 10.1016/j.gendis.2024.101241.
20. Y. Gu, Y. Hu, H. Zhang, S. Wang, K. Xu, and J. Su, "Single-cell RNA sequencing in osteoarthritis," *Cell Prolif.*, Dec. 2023; 56(12): e13517. doi: 10.1111/cpr.13517.
21. Z. Deng *et al.*, "TGF-β signaling in health, disease and therapeutics," *Signal Transduct. Target. Ther.*, Mar. 2024; 9(1): 61. doi: 10.1038/s41392-024-01764-w.
22. P. Sengprasert, O. Kamenkit, A. Tanavalee, and R. Reantragoon, "The Immunological Facets of Chondrocytes in Osteoarthritis: A Narrative Review," *J. Rheumatol.*, 51 Jan. 2024; 13–24. doi: 10.3899/jrheum.2023-0816.
23. J. Zhang *et al.*, "The role of HIF-1α in hypoxic metabolic reprogramming in osteoarthritis," *Pharmacol. Res.*, Mar. 2025; 213: 107649. doi: 10.1016/j.phrs.2025.107649.
24. Z. Wen *et al.*, "The role of Th/Treg immune cells in osteoarthritis," *Front. Immunol.*, Sept. 2024; 15: 1393418. doi: 10.3389/fimmu.2024.1393418.
25. M. Lu, M. Zhu, Z. Wu, W. Liu, C. Cao, and J. Shi, "The role of YAP/TAZ on joint and arthritis," *FASEB J.*, 38(10): e23636, May 2024, doi: 10.1096/fj.202302273RR.